Fluid Motion for Microgravity Simulations in a Random Positioning Machine

Carole A. D. Leguy[1], Rene Delfos[1], Mathieu J.B.M. Pourquie[1], Christian Poelma[1], Janneke Krooneman[2], Jerry Westerweel[1] , and Jack J.W.A. van Loon[3]

[1] Laboratory for Aero and Hydrodynamics, Delft University of Technology, (NL); [2] Bioclear, Groningen (NL); [3] DESC @ OC, Academic Centre for Dentistry Amsterdam (NL)

BACKGROUND

To understand the role of gravity in biological systems one may decrease inertial acceleration by going into free-fall conditions such as available on various platforms. These experiments are cumbersome and expensive. Thus, alternative techniques like Random Positioning Machines (RPM) are now widely used to simulate the micro-gravity environment (Yuge et al., 2003; Borst and van Loon, 2009; Pardo et al., 2005). These instruments generate random movements so that cumulative gravitational effects cancel out over time. However, comparative studies performed with the RPM and culture cells were unable to reproduce the spaceflight results (Hoson et al., 1997). These differences may be explained by stresses acting on the culture cells in an RPM whereas these stresses are not present in microgravity conditions. They may be caused by internal fluid motion, originating from instationary rotation. The aim of this study is to quantify fluid flow behavior and wall shear stresses (as they are relevant to cells cultured at the flask wall), and internal shear stresses as they are relevant to suspended (free-floating) cells in an RPM container. We do this both experimentally using Particle Image Velocimetry (PIV) and numerically using 3D Direct Numerical Simulation (DNS) of the flow.

METHODS

A dual-axis rotating frame machine is used to reproduce the motion of a real RPM in a controllable way according to a pre-programmed motion protocol. A flask filled with fluorescent tracer particles (d=13 μm, ρ=1150 kg/m^3) and water with sodium chloride of the same density as the particles is positioned at the center of rotation, where it is surrounded by a co-rotating 2-component planar PIV system (Adrian and Westerweel, 2011), see Figure 1. A green light dye-laser of 534 nm wavelength is used to create a light sheet inside the flask. We use a double-frame camera to record the particles inside the flask. The motor motion is generated with a servo-control system up to a maximum angular speed of 30º/s, and acceleration up to 60º/s^2. Images are recorded at a maximum frequency of 15 Hz for a duration of typically 30s corresponding to 6 motion cycles.

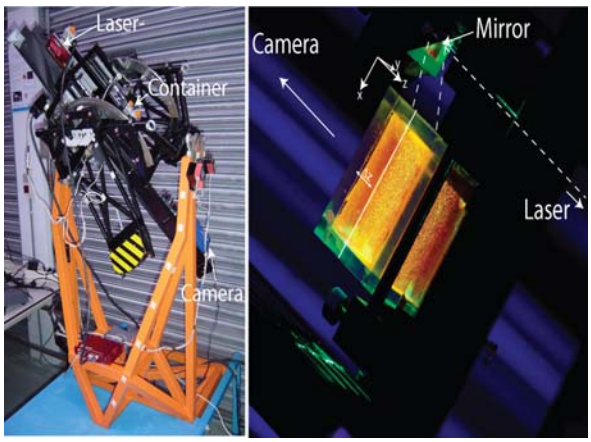

Figure 1. Left: Particle Image Velocimetry system mounted on a two-axis rotating frame. Right: Detailed view of the container. A light sheet is created in the XY plane at a distance Δz from the container wall.

The same experiment is simulated numerically using an existing DNS model (Pourquié, 2009) to which the effect of rotation is added by implementing extra body forces (angular acceleration, centrifugal, Coriolis) to the momentum equation, including the motion protocol as applied to the experiment. The simulation has sufficient spatial and temporal resolution to fully resolve the flow field. The (rectangular) flask geometry equals the one used for the experimental study (65 x 40 x 20 mm^3).

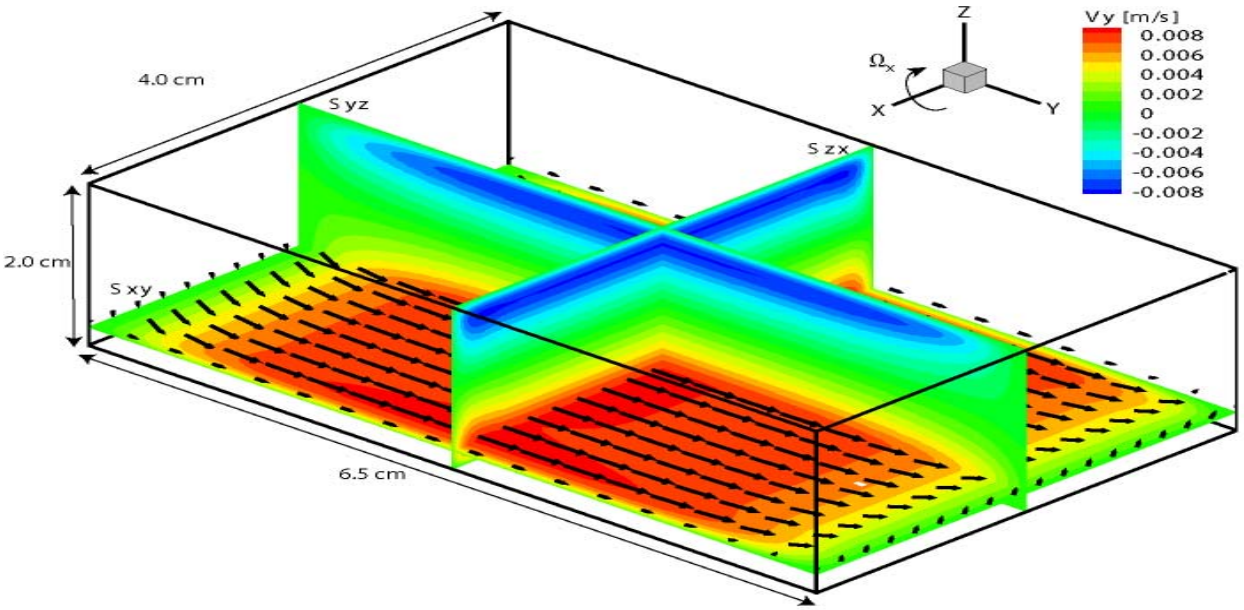

Figure 2. Simulated velocity field in the y direction (t-6.3 s) with slice view of the XY, YZ and ZX planes.

RESULTS

For a periodic and sinusoidal rotation around a single axis, fluid motion induced by inertia is observed parallel to the wall; see Figure 2 and 3. The RMS-average difference between the simulated and measured velocity field is equal to 0.5 mm/s, or 6% of the maximum velocity. The quantitative result demonstrates the good agreement between the simulated and the measured velocity profiles.

In Figure 3, measured and simulated velocities at the center of the measurement plane are depicted as a function of time. It can be seen that a periodic state is reached after only one period. The time evolution of the velocity profiles is shown on Figure 4 for the velocity in the y direction V_y. The increase and decrease of V_y along the y direction due to the circulation in the container can be seen. Along the x-axis of rotation, the profile is flat (i.e. 2D flow), except for end-effects (boundary layers) near the flask wall. Since the PIV measurements provided the velocity field only over the XY plane at a (fixed) distance of 3.3 mm from the wall, the 3-D simulated results are used to study the velocity profile along the *z* axis. The evolution of the boundary layer can be seen near the flask wall. A maximum wall shear stress of 6.2 mPa is obtained with an angular phase shift of 54 degree with respect to the angular velocity of the rotating axis.

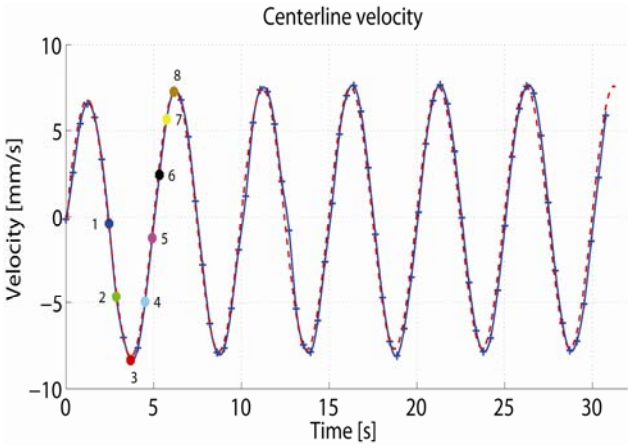

Figure 3. Velocity in the Y direction at the center of the z = 3.3 mm plane obtained for the measurements (in blue) and from simulated data (in red).

For spin-up about 2 axes according to the instationary angular velocity used in a commercial RPM (see Figure 5), more complex patterns are obtained in the DNS. A maximum velocity up to 70 mm/s near the wall and a maximum stress at the container wall of 62 mPa are derived.

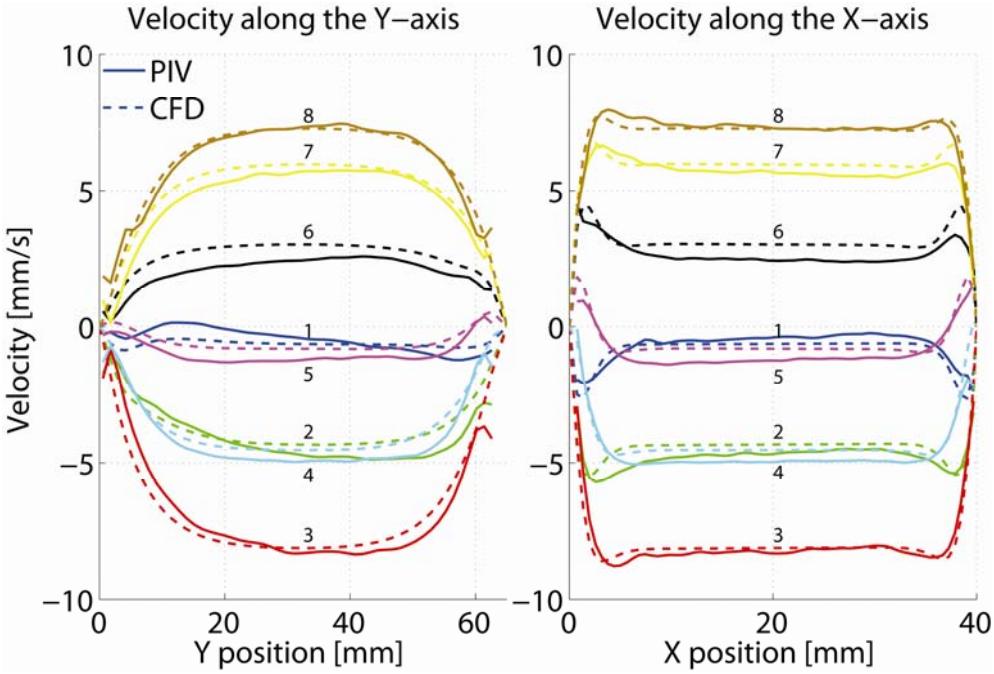

Figure 4. Comparison between the simulated and measured velocity profiles at several time steps as a function of Y position, at the intersection of the S_{xy} and S_{yz} plane (left), and as a function of the x position at the intersection between the Sxy and Szx planes (right).

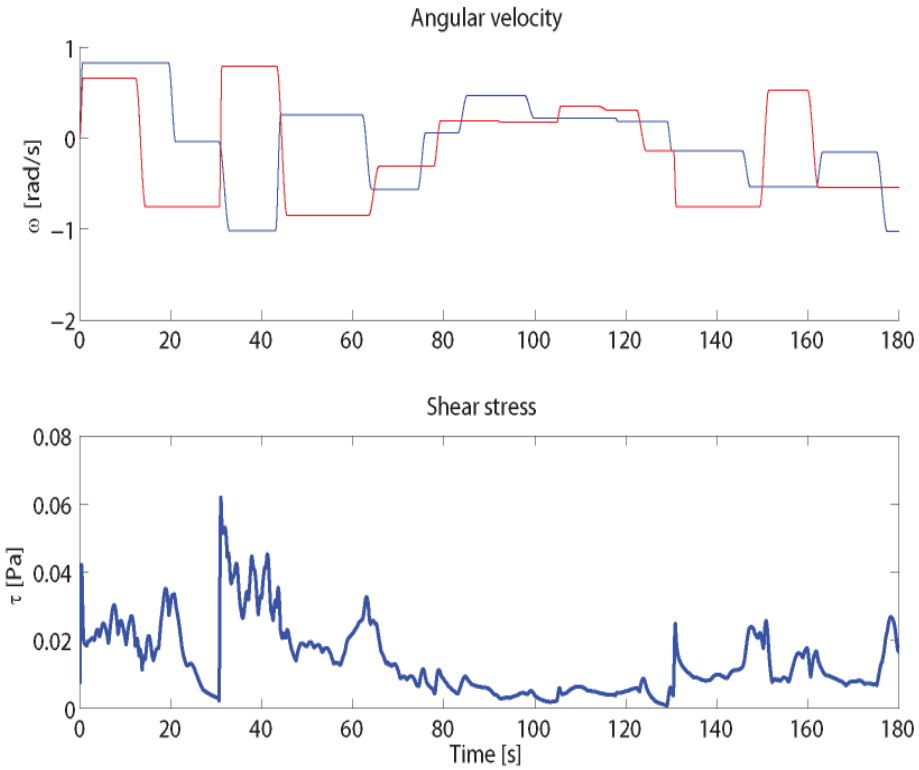

Figure 5. Angular velocity patterns for both axes (top), maximum wall shear stress (bottom) according to the angular velocity used in an RPM. Box-size: 6 × 4 × 2 [*cm*].

CONCLUSION

For sinusoidal rotation, quantitative agreement between simulated and measured velocity field has been found which is considered as a validation of the numerical model. Considering motions as are employed for an RPM, the numerical study suggests that stresses induced by the fluid are particularly high during changes of rotation velocity, i.e. acceleration. In the near future, we aim to provide a quantitative comparison between experimental and numerical results for dual axis motion. Furthermore, we are developing a user protocol for the RPM users.

REFERENCES

Adrian R.J. and Westerweel J. 2011. *Particle image velocimetry*. Cambridge University Press.

Borst A. and van Loon J. 2009. Technology and Developments for the Random Positioning Machine, RPM. *Microgravity Science and Technology 21:* 287–292.

Hoson T., Kamisaka S., Masuda Y., Yamashita M., and Buchen B. 1997. Evaluation of the tree-dimensional clinostat as a simulator of weightlessness. *Planta* 203: S187-S197.

Pardo S.J., Patel M.J., Sykes M.C., Platt M.O., Boyd N.L., Sorescu G.P., Xu M., van Loon J.J., Wang M.D., and Jo H. 2005. Simulated microgravity using the Random Positioning Machine inhibits differentiation and alters gene expression profiles of 2T3 preosteoblasts. *American Journal of Physiology. Cell Physiology* 288(6): C1211–C1221.

Pourquié M.J.B.M. 2009. Accuracy Close to the Wall of Immersed Boundary Method, proc. 4th European conf. of the Int. feder. for med. and biol. Eng. IFMBE. Volume 22, Part 14, 1939-42, DOI: 10.1007/978-3-540-89208-3_462

Yuge L., Hide I., Kumagai T., Kumei Y., Takeda S., Kanno M., Sugiyama M., and Kataoka K. 2003. Cell differentiation and p38 (MAPK) cascade are inhibited in human osteoblasts cultured in a three-dimensional clinostat. *In Vitro Cell Dev. Biol. Anim. 39:89-97*